© 2021. Published by The Company of Biologists Ltd | Journal of Experimental Biology (2021) 224, jeb242167. doi:10.1242/jeb.242167

RESEARCH ARTICLE

The routes of one-eyed ants suggest a revised model of normal route following

Joseph L. Woodgate[1], Craig Perl[2,*] and Thomas S. Collett[2,‡]

ABSTRACT

The prevailing account of visually controlled routes is that an ant learns views as it follows a route, while guided by other path-setting mechanisms. Once a set of route views is memorised, the insect follows the route by turning and moving forwards when the view on the retina matches a stored view. We engineered a situation in which this account cannot suffice in order to discover whether there may be additional components to the performance of routes. One-eyed wood ants were trained to navigate a short route in the laboratory, guided by a single black, vertical bar placed in the blinded visual field. Ants thus had to turn away from the route to see the bar. They often turned to look at or beyond the bar and then turned to face in the direction of the goal. Tests in which the bar was shifted to be more peripheral or more frontal than in training produced a corresponding directional change in the ants' paths, demonstrating that they were guided by the bar. Examination of the endpoints of turns towards and away from the bar indicate that ants use the bar for guidance by learning how large a turn-back is needed to face the goal. We suggest that the ants' zigzag paths are, in part, controlled by turns of a learnt amplitude and that these turns are an integral component of visually guided route following.

KEY WORDS: Ant navigation, Rapid turns, Visually guided routes

INTRODUCTION

Foraging ants, with their faculties intact, readily learn and follow visually guided routes between their nest and a foraging site (Collett et al., 1992; Wehner et al., 1996; Collett, 2010; Mangan and Webb, 2012; Narendra et al., 2013). They can do so despite a large mismatch between their position on the route and their path integration (PI) state (Kohler and Wehner, 2005; Graham and Cheng, 2009; Narendra et al., 2013), implying that visual guidance does not require support from PI, even though the two guidance mechanisms are normally co-active (Collett, 2012; Wehner et al., 2016; Hoinville and Wehner, 2018). Such experiments and modelling (Baddeley et al., 2012) supported the idea that visual route following involves 'alignment image matching' (for reviews, see Zeil, 2012, Collett et al., 2013). In brief, ants that are guided initially by PI and by innate responses to obstacles and visual features that they encounter along the way, memorise routes by recording retinotopic views when facing along the route. Thereafter, they can follow the route by turning until they face in the direction that best matches an item from their set of recorded views and then walk forward (Baddeley et al., 2012).

We report here experiments on one-eyed ants learning short routes in the restricted surroundings of a laboratory, in which celestial compass information was lacking. The results suggest that there are probably additional mechanisms to visual route learning. Our experiments were stimulated by earlier work (C. Buehlmann, T.S.C., P. Graham and J. E. Niven, unpublished data) in which ants with one eye painted over were trained to find a drop of sucrose at the edge of a circular arena. The ants were released at the centre of the arena and learnt a straight route from there to a point on the circumference. This location was specified by a black vertical bar fixed to the white inner wall of a rotatable cylinder surrounding the arena. When the ants faced along the route, the bar was well outside the visual field of the ants' seeing eye (e.g. Zollikofer et al., 1995). The cylinder and the position of the food were rotated together from trial to trial to ensure that the black bar was the principal visual cue and also to remove any reliance on a magnetic compass (Çamlitepe and Stradling, 1995). Ants with their left eye capped were approximately normal in route learning when the bar was on the right side of the route going from the centre to the periphery of the arena, but struggled when the shape was on the left side (C. Buehlmann, T.S.C., P. G. Graham and J. E. Niven, unpublished data).

From the perspective of image alignment, this failure is not surprising. To the one-eyed ant, the view along the desired route is of an empty cylinder (Fig. 1A) and the ant can fulfil this condition by picking from a wide swath of possible paths. One possible solution to the problem, which does allow continuous visual control, is to walk sideways while facing the cue (Fig. 1B). Ants do not adopt this strategy. Instead, they exhibit behaviour which indicates that the standard model of alignment image matching may be supported by other mechanisms.

In the present study, we followed the same procedure, except that we added extra information that seemed to help some ants learn a route (Fig. 1C). Ants were pointed in the direction of the food at the start of the route by two short parallel strips of wood aligned along the route.

MATERIALS AND METHODS

Ants

Experiments were performed, in 2017, on wood ants (*Formica rufa* Linnaeus 1761) from laboratory-maintained colonies collected from Broadstone Warren, East Sussex, UK. The colonies were kept under a 12 h:12 h light:dark cycle and the colony was sprayed with water daily. Water and sucrose dispensers were always available except during experiments when the colony had limited access to sucrose to encourage enthusiastic foraging. Frozen crickets were supplied several times a week.

[1]School of Biological and Chemical Sciences, Queen Mary University of London, London E1 4NS, UK. [2]School of Life Sciences, University of Sussex, Brighton BN1 9QG, UK.
*Present address: Department of Zoology: Functional Morphology, Stockholm University, Svante Arrhenius väg 18b, 106 91 Stockholm, Sweden.

‡Author for correspondence (t.s.collett@gmail.com)

J.L.W., 0000-0001-8176-7024; C.P., 0000-0002-9911-1207; T.S.C., 0000-0001-9548-5861

Received 22 December 2020; Accepted 12 July 2021

Journal of Experimental Biology (2021) 224, jeb242167. doi:10.1242/jeb.242167

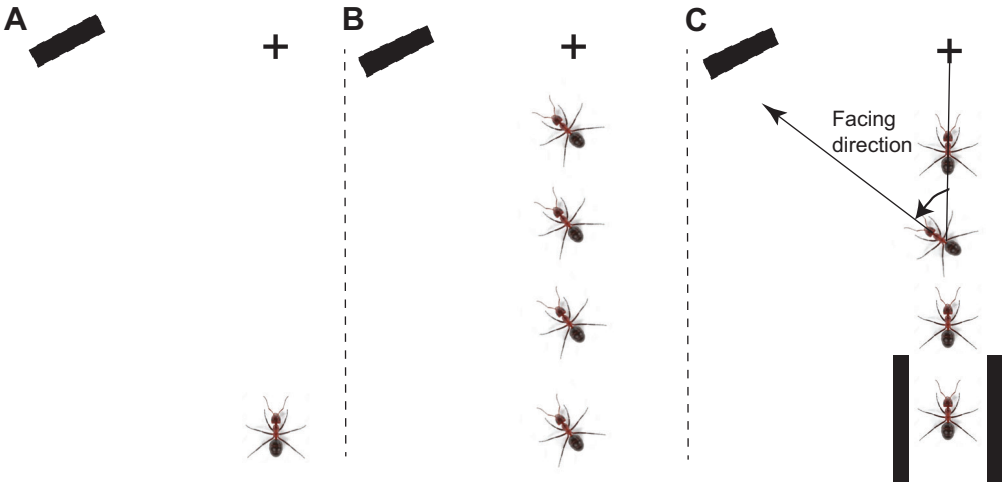

Fig. 1. Schematic of problem and solution. (A) Ant with left eye covered has difficulties in reaching its goal when the only directional aid is a black, vertical stripe outside the right eye's visual field. (B) Ant could, but does not, approach the goal by moving sideways. (C) Ant is aided by mechanical guides forming a channel at the start of the route. While on the route, it turns to face towards and then away from the stripe. Facing direction is defined in the Materials and Methods. Right turns of the appropriate size help the ant keep to the route and reach the food (+).

Before ants were trained, each left eye was painted with enamel paint and the integrity of the paint cover checked daily under a binocular microscope. The cover appeared stable and it was very rare to have to repaint.

Experimental set-up

The basic experimental procedures followed those described previously (e.g. Lent et al., 2013). Individually marked wood ants were trained to go from the centre of a circular platform (radius 60 cm) towards a drop of sucrose on a microscope slide placed 55 cm from its centre. The slide was positioned relative to a single black vertical bar (50 cm wide and 85 cm high) that was cut from black cotton sheeting and fixed to white netting on the white inner wall of a rotatable cylinder (diameter 3 m, height 1.8 m). Seen from the centre of the arena, the right edge of the bar was 45 deg to the left of the direction of the sucrose.

To provide idiothetic cues, a pair of guide sticks (3 mm square cross-section, pale balsa wood, the 10 cm ones painted white) with a 24 mm path between them led from an exit gap in the ring (10 cm diameter and 2.5 cm high) surrounding the centre of the arena. In initial training trials, the sticks led most of the way to the food, their length was gradually shortened to 13 cm. 10 cm and 13 cm sticks were used for tests. See Fig. 3 for a top view of the arena, the arrangement of sticks, the sucrose and the radial position of the bar.

Experimental procedure

Ants were given ∼25 trials of group training over ∼3 days before being trained individually. On each trial, individually marked ants from a cohort of ∼25, were taken from the nest and separated into groups of 6–8 individuals. One group at a time was placed inside the 10 cm ring, sometimes overlapping with stragglers from a previous group. After the ants had reached the feeder and had started to drink, they were placed in a box with sucrose and drank their fill before being returned to the nest.

For individual training and tests, ants were put singly into a 6.5 cm diameter, cylindrical holding chamber that lay within the ring. The wall of the holding chamber was lowered remotely from outside the cylinder so it was flush with the arena floor. Once the wall was lowered the ant was free to leave the ring. When the ant had reached the food reward and started to feed, or reached the edge of the arena, the experimenter raised the wall of the holding chamber, entered the cylinder, transferred the ant to a feeding box and placed the next ant in the holding chamber. After the cohort of ants had completed a training trial, the guide sticks, the black bar and the slide with food were rotated to a new position to avoid the ants learning other cues for guidance.

Once individual training began, we recorded each ant's path, starting just before the ant was released from the holding chamber. The ant's movements were recorded using a tracking video camera (Trackit, SciTrackS GmbH), which gave as output the ant's position on the arena and the orientation of its body axis every 20 ms. Each ant was released from the holding chamber and its path recorded until it reached the sucrose or the edge of the platform. Once it had started to feed, or if it failed to reach the sucrose within a couple of minutes, it was placed in a feeding box in which there was sucrose on a microscope slide.

After individuals had performed 30 training trials, three different tests were introduced with a varying number of intervening training trials. In test 1, the right edge of the bar was shifted to 90 deg to the left of the direction in which the starting channel was pointing. In test 2, the bar was shifted in the opposite direction, ∼5 deg to the left of the channel direction. In test 3, the bar was removed. No sucrose reward was present during tests. Ants were removed from the arena once they reached the edge of the platform and allowed to feed before they were returned to the nest.

Data analysis

We examined three features of an ant's trajectories: (1) the overall direction of its path; (2) a measure of the overall sinuosity of each path; (3) the ant's facing direction at the extrema of its turns to the left and the right, measured relative to the position of the food. Path directions and facing directions at turn endpoints were computed by projecting the ant's body orientation to the point at which it intersected the edge of the platform. The facing direction was then given by the angle between the line connecting the centre of the arena to the projection point and that connecting the centre of the arena to the location of the food.

In Figs 2–7 and Figs S3–S4, the angular position of the bar relative to the ant's body orientation is depicted as though the ant were at the centre of the arena. Since facing directions are computed independently of what the ant sees, the direction of the ant's path as shown on the x-axis of the figures is unaffected by this approximation of the retinal position of the bar. The consequent errors in the retinal position of the bar are not large. If the ant were to decide on its route on leaving the channel, i.e. 18 cm from the centre, the position of the bar would be only 5.3 deg different from its position as seen from the centre of the arena and would shift by

Journal of Experimental Biology (2021) 224, jeb242167. doi:10.1242/jeb.242167

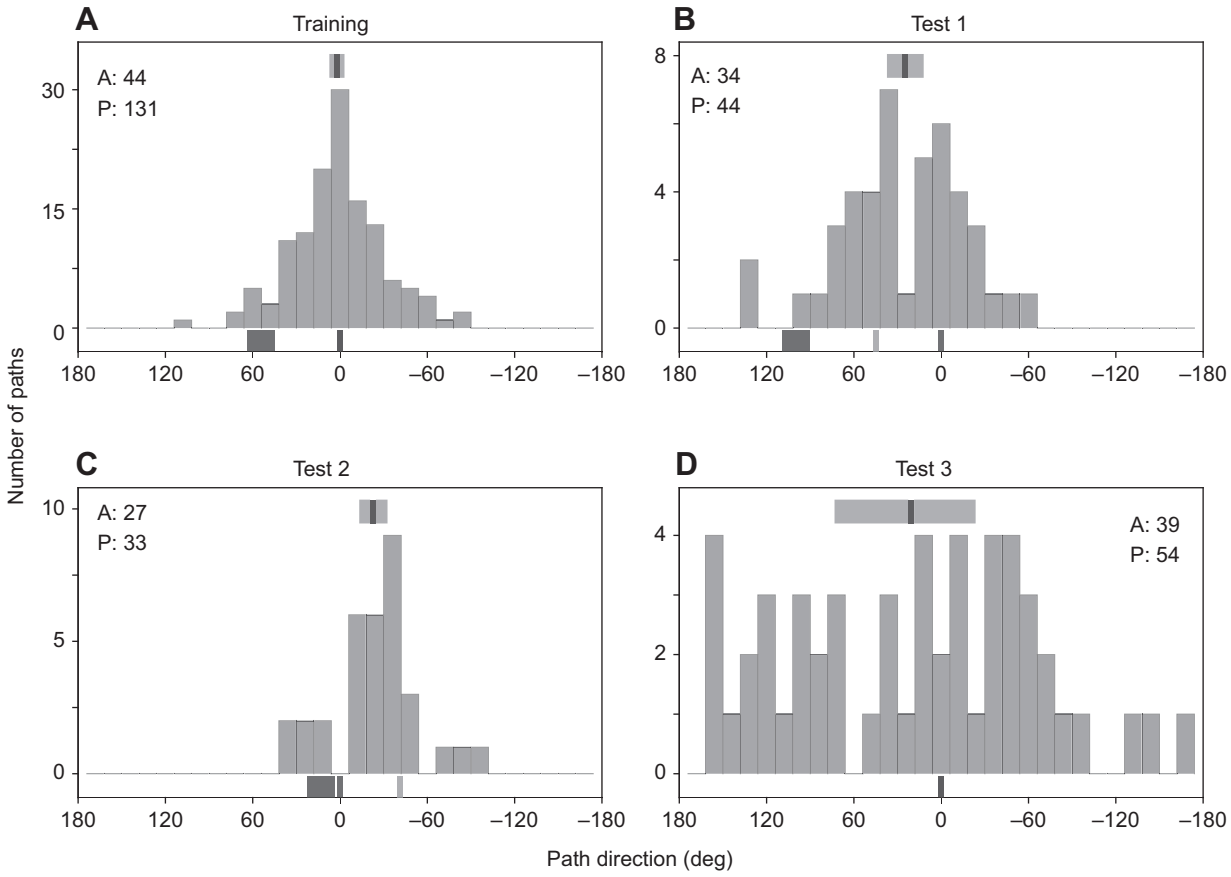

Fig. 2. The path directions of one-eyed ants during training and tests. Path directions during training and three tests (see the Materials and Methods). (A) Histogram showing the overall path directions taken by ants in training trials immediately preceding a test. Bin width is 12 deg; 0 deg is the feeder direction and is marked by a black line below the histogram; positive angles are counter-clockwise. A is the number of ants and P is the number of paths; the black line and grey rectangle above the histogram show the mean and 95% confidence intervals of the distribution; the black rectangle below the histogram shows the width and position of the bar as seen from the centre of the arena. These conventions hold across all figures. (B) Path directions in tests with bar shifted left of its training position. Path direction is taken as the ants' facing direction relative to the feeder direction at 0 deg (black line). Grey line shows the predicted feeder direction assuming use of the bar for guidance. (C) Path directions in tests with the bar shifted to the right. (D) path directions in the absence of the bar. Rayleigh's tests for non-uniformity were all significant (pre-test training: Z=36.2, P<0.001; test 1: Z =20.3, P<0.001; test 2: Z =20.2, P<0.001; test 3: Z =3.48, P=0.030). Hartigan's dip test was only significant for test 1 (pre-test training: N=44, dip statistic=0.032, P=0.996; test 1: N=33, dip statistic=0.05, P=0.046; test 2: N=26, dip statistic=0.05, P=0.971: test 3: N=36, dip statistic=0.04, P=0.963).

just another 9.8 deg on its path to the feeder. That also applies to the endpoint histograms in Fig. 4.

Path direction

The direction of the ants' paths was analysed from when an ant left the guide channels, beginning ∼18 cm from the centre of the arena, or sooner if ants climbed over the guide strips, until they reached a radial distance of 45 cm from the centre. The direction over this path-segment was estimated in two stages. First, the path (consisting of x–y coordinates recorded at 50 fps) was divided into successive 1.5 cm segments, and orthogonal distance regression (Golub and van Loan, 1996) was used to calculate the angle of a best fit line through each segment, minimising the error in both x and y dimensions (custom written MATLAB script based an algorithm devised by T. Eitan: https://stackoverflow.com/questions/12250422/orthogonal-distance-regression-in-matlab). The best fit line was projected forward to determine where it intersected with the edge of the platform. The overall direction of the path was then taken to be the circular mean of the facing directions of all path segments until the ant's path took it 45 cm from the centre of the arena.

Sinuosity

For each path, we calculated the ratio of the ant's distance travelled (cumulative sum of straight-line distances between all consecutive positions of the ant) to the straight-line distance between the start and end of the track. A score of 1 would indicate a perfectly straight track, while higher scores indicate a more meandering or sinuous path.

Turns and their endpoints

Plots of facing directions over time have inflection points that are linked to the ant's zigzag path along the route. The facing direction at these points was defined as the most extreme angle to the left or right before a change in the direction of rotation. These extrema or 'turn endpoints' were identified using the following procedure: first, to reduce noise in the data, the ant's facing direction throughout each track was smoothed by taking the circular mean facing direction across a 50-frame moving window. Points at which the angular change between consecutive frames reversed direction gave the rough location of inflection points in the track. To pick out the facing direction just prior to a reversal of direction, we used the unsmoothed angle data to find the interval over which the facing

Journal of Experimental Biology (2021) 224, jeb242167. doi:10.1242/jeb.242167

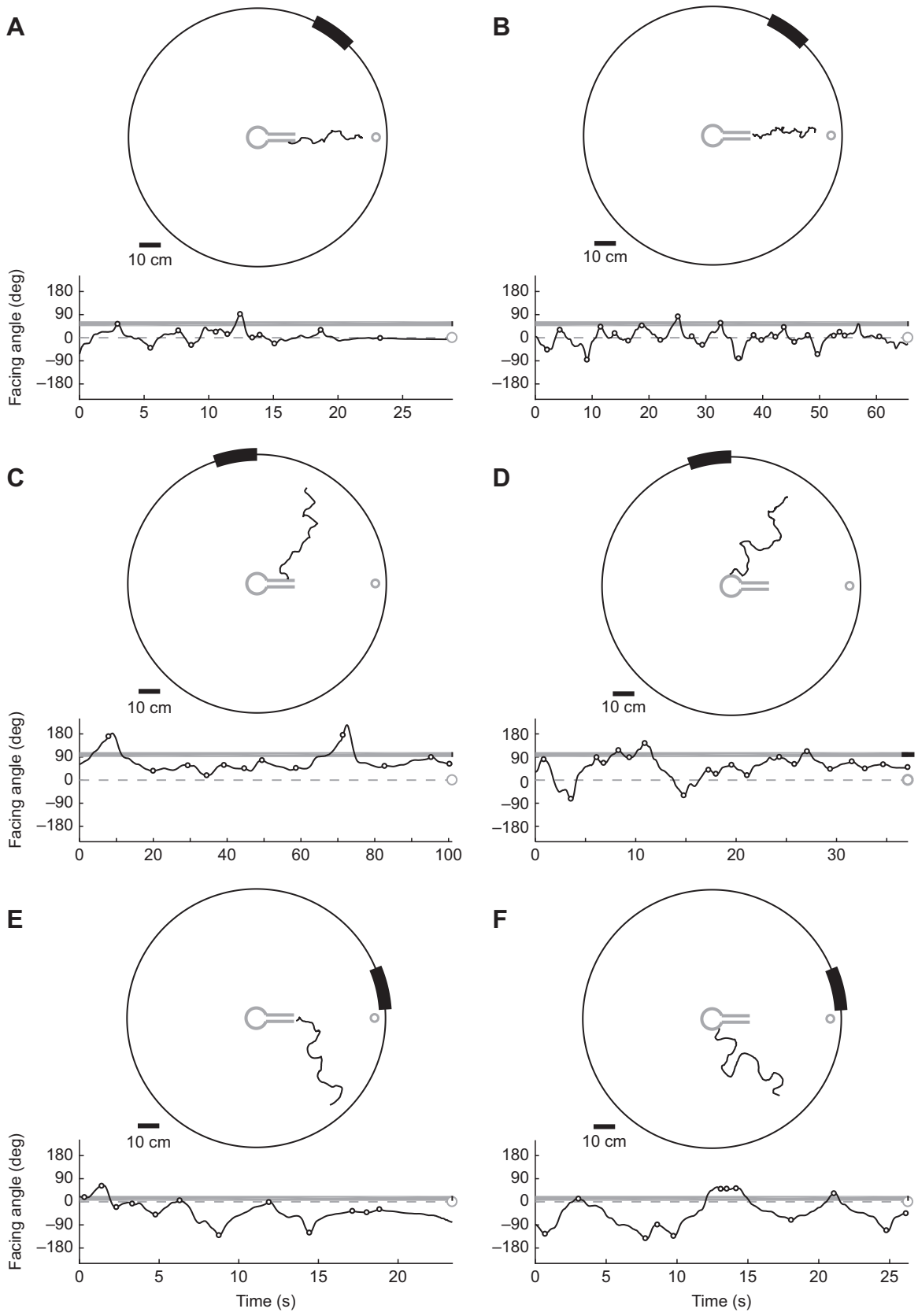

Fig. 3. Individual examples of ants' trajectories during training and tests to illustrate turn endpoints. (A,B) Training paths. (C–F) Tests with bar shifted leftwards (C,D) or rightwards (E,F) from the training position with no food present. Each panel shows the path of a single ant. Top: path of each ant, seen from above, as it moves from the enclosure and guiding channel in the centre of the arena towards the food position (open circle; 0 deg) 55 cm away. Black bar on circumference of arena is the projection of the vertical bar that is fixed to the surrounding 180 cm diameter cylinder. Bottom: Ant's facing direction plotted against time from the start of the illustrated trajectory. Dashed line at 0 deg is the feeder direction. Gray bar shows angular position of bar as measured from arena centre. Circles mark extracted turn extrema.

Journal of Experimental Biology (2021) 224, jeb242167. doi:10.1242/jeb.242167

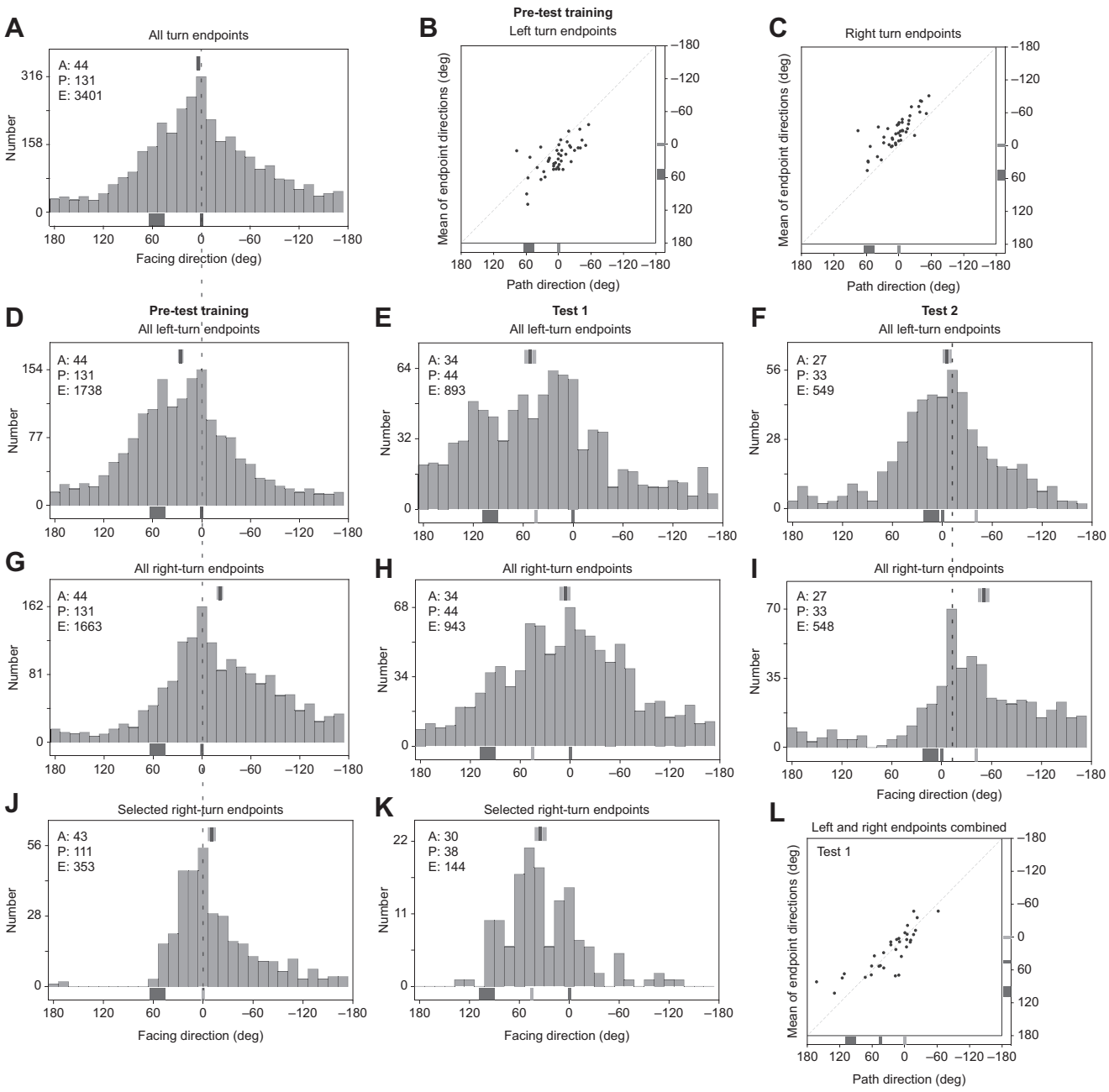

Fig. 4. The endpoints of turns. (A) Facing directions of left and right turn endpoints in pre-test training runs. The mean of the distribution does not differ significantly from the feeder direction (mean: 0.99 deg CI: −7.3 to 8.8 deg; Likelihood ratio test: χ^2_1=0.81, P=0.814). E denotes number of endpoints. Other details in all histograms are as in Fig. 2. (B,C) Correlation between mean path direction and the means of all left (B) and right (C) turn endpoints across all the pre-test training trials performed by each ant (N=44 ants). Dashed diagonal line supposes alignment of mean endpoints with path directions. Mean of left turn endpoints correlate with path directions (B; circular correlation coefficient ρ=0. 69: P<0.001), but fall to their left (mean difference: 22.8 deg 95% CI: 16.3 deg to 29.3 deg; Likelihood ratio test: χ^2_1=30.51, P<0.001). Mean right turn endpoints correlate with path directions (C; circular correlation coefficient ρ=0. 81: P<0.001), but fall to their right (mean discrepancy: −27.6; 95% CI: −32.9 to −22.2 deg; Likelihood ratio test: χ^2_1=52.6, P<0.001). (D–F) Left turn endpoints in (D) pre-test training where mean of endpoints (24.3 deg CI: 16.3 to 32.7 deg) differs from feeder direction (Likelihood ratio test: χ^2_1=25.0, P<0.001); (E) test 1, where mean endpoint (51.5 deg CI: 37.8 deg to 65.0 deg) differs from feeder direction but not from bar-defined direction (Likelihood ratio test, channel direction: χ^2_1=28.5, P<0.001; bar-defined direction: χ^2_1=0.63, P=0.427); (F) test 2, where mean endpoint (7.4 deg CI: −6.3 to 20.4 deg) does not differ from feeder direction, but differs from bar-defined direction (Likelihood ratio test, feeder direction: χ^2_1=2.06, P=0.151; bar-defined direction: χ^2_1=26.4, P<0.001). (G–I) Endpoints of all right turns in (G) pre-test training, where mean endpoint differs from feeder direction (−24.9 deg, CI: −34.1 to −16.0 deg; Likelihood ratio test: feeder direction: χ^2_1=22.4, P<0.001); (H) test 1, where mean endpoint does not differ from feeder direction, but differs from bar-defined direction (2.1 deg, CI: −14.5 to 19.7 deg; Likelihood ratio test, feeder direction: χ^2_1=0.01, P=0.914; bar-defined direction: χ^2_1=17.3, P<0.001); (I) test 2, where mean endpoint differs from feeder direction but not from bar-defined direction (−54.4 deg, CI: −68.2 to −40.7 deg; Likelihood ratio test, feeder direction: χ^2_1=27.3, P<0.001; bar-defined direction: χ^2_1=2.5, P=0.112), respectively. All means shift to the right of their companion left turn endpoints. (J,K) Endpoints of right turns that start within ±20 deg of the centre of the bar in (J) pre-test training, where mean turn endpoints differ from feeder direction (−15.9 deg CI: −24.2 to −7.8 deg; Likelihood ratio test, feeder direction: χ^2_1=9.00, P=0.003) and (K) test 1, where mean turn endpoints differ from feeder direction but not from bar-defined direction (30.5 deg CI: 17.9 to 43.0 deg; Likelihood ratio test: feeder direction: χ^2_1=10.2, P=0.001; bar-defined direction: χ^2_1=3.15, P=0.076). (L) Correlation of the means of all left plus right turn endpoints made in test 1 by each ant with that ant's corresponding mean path direction. Vertical dashed lines connecting panels A,D,G,J, and F and I emphasise alignment of the peak values of these distributions.

direction was more extreme than the facing direction at the inflection point. The mid-point of this interval was taken as the facing direction at the turn endpoint.

The algorithm used to extract extrema occasionally does not capture all the turn endpoints that can be seen by eye (e.g. Fig. 3), because some turns were too small for the inflection point to show up in the smoothed angle data. We saw no indication of false identification of extrema.

Some turns end in a clear plateau rather than a turn in the opposite direction. When this was the case, the ant's facing directions at these plateaux were also considered to be turn endpoints. Plateaux were identified through the fulfilment of two criteria: (1) an interval during a track that lasted at least 0.2 s, in which the maximum change in facing directions was less than 3 deg; (2) that the slope of the regression of facing direction against time of a candidate plateau should be less than 1 deg s^{-1}. The facing direction of an identified plateau was then defined as the circular mean of all facing directions in the interval.

Exclusion of inconsistent ants

Some ants were very erratic. Paths of these ants are included in Fig. S1 but excluded from further analyses. To remove these ants, we calculated the overall direction of travel of each path from every ant and calculated the resultant vector length of the path directions of each ant across the entire training period. Ants whose resultant vector length was >0.4 took similar directions relative to the visual and idiothetic cues in each trial, despite the rotation of the experimental arena. Those with a vector length <0.4 did not appear to have learned a route; 5 such ants were removed from the training and test dataset. One of these 5 had taken part in tests 1 and 2, and none had participated in test 3.

A small number of ants were tested but had not taken part in the training trial immediately preceding the test. Data from these ants are included in histogram figures showing path directions and turn endpoints but were excluded from the statistical analysis to ensure that we only tested ants that had recent experience with the training set-up. Thus, one ant was excluded from analyses of test 1, one ant from test 2, and three ants from test 3.

Statistical methods

Much of the data are presented as histograms of the ants' path directions and endpoints in training and in tests 1–3. Each of these distributions was tested for uniformity using Rayleigh tests (test described by Fisher, 1995; MATLAB implementation, CircStat; Berens, 2009). All distributions were significantly non-uniform (all $P<0.0001$) and were then tested for unimodality, using Hartigan's dip test that identifies deviations from unimodality (Hartigan and Hartigan, 1985; MATLAB code written by F. Mechler; https://gist.github/schluppeck/e7635dcf0e80ca54efb0). To do so, circular distributions were first 'unwrapped' by cutting them at a point opposite the circular mean. This procedure does not affect the location of potential modes as each distribution had few observations in the quadrant opposite to the mean.

Note that histograms of path directions show the headings of all paths of a specified type, but, when an individual ant contributed more than one path to a histogram, the statistical analyses used the circular mean direction of all the ant's paths. Similarly, histograms of turn endpoints show all recorded endpoints, but the statistical analyses were applied to the circular mean of all endpoints made by an individual ant.

At the top of each histogram are shown the circular mean of the distribution (black line) and the 95% confidence intervals (calculated using the likelihood-based arc method after bootstrapping 10,000 times).

The mean path direction or endpoint facing direction was compared with the feeder direction or approximate bar-defined direction using the likelihood ratio test (test described by Mardia and Jupp, 2009; custom MATLAB code written by J.L.W.). We compared the mean path direction or endpoint direction in tests to that in training using the two-sample Watson–Williams test, a circular analogue of the two-sample *t*-test (test described by Watson and Williams, 1956; MATLAB implementation, CircStat, Berens, 2009).

There was a significant correlation between the mean direction of all endpoints (or all left-turn or right-turn endpoints) by each ant and the mean path heading direction of the same ant, as shown by calculating the circular correlation coefficient (as in Jammalamadaka and Sengupta, 2001) with MATLAB (Berens, 2009). To examine whether the endpoints differed significantly from the heading direction, we calculated the discrepancy between each mean endpoint direction and the corresponding path direction and tested whether the mean discrepancy differed from zero using likelihood ratio tests. The probability values given by all likelihood ratio and Watson–Williams tests were two-tailed.

RESULTS

The paths of monocular ants

The individual paths of all ants during training runs, and in tests in which the black bar on the cylinder wall was shifted or removed, were widely spread, with the centre of gravity and concentration shifting with the different tests (Fig. S1). In this population, 5 out of the 49 ants were so inconsistent during training that they were excluded from further study (see Materials and Methods). For an initial analysis of the behaviour of the remaining 44 ants, the directions of their paths were plotted relative to the 'feeder direction', i.e. the direction from the centre of the arena along the starting channel to the feeder or in tests to the feeder's virtual position. Path direction was computed in a way that made the facing direction independent of the bar's position on the ant's retina (see Materials and Methods). The histograms in Fig. 2 show the mean facing direction of each ant along the first 45 cm of its path. The position of the bar in all figures is depicted as though the ant were in the centre of the arena. These histograms and those in all subsequent figures were tested for uniformity. In every case, Rayleigh's test for non-uniformity was significant (see Fig. 2 legend). All the histograms were also tested for unimodality with Hartigan's dip test. To avoid pseudo-replication, statistical analyses relied on the circular mean of all paths of each individual ant as the dependent variable.

The mean heading of the paths in the training trials before a test (Fig. 2A) was close to the feeder direction and did not differ significantly from it (circular mean: 0.81 deg; 95% confidence interval for the mean (CI): −6.89 deg to 7.97 deg; Likelihood ratio test, $\chi^2_1=0.043$, $P=0.835$). Many individual paths lay close to the feeder direction: the directions of 30 paths of 19 ants lay within ±6 deg of the feeder direction. The numbers grew to 45 paths from 24 ants and 66 paths from 34 ants, as the sample width was increased to ±12 deg and ±18 deg, respectively. Without the possibility of alignment image matching, this successful route following is perhaps more surprising than its failure.

Tests in which trained ants were tested with the bar displaced to the left or to the right of its training position demonstrate that the ants' direction of travel shifts with the displacement, indicating that routes to the feeder in training are in part guided by the bar. In test 1,

the right edge of the bar was 90 deg counter-clockwise from the feeder direction (Fig. 2B, Fig. S1B). Hartigan's dip test confirms that the histogram of path headings was bimodal with peaks in the bar-defined and feeder directions (Fig. 2B). The mean heading was 24.4 deg (CI: 10.8 to 37.9 deg) and lay between the feeder and bar-defined directions, differing significantly from both (Likelihood ratio test: channel direction: χ^2_1=9.53, P=0.002; bar-defined direction: χ^2_1=7.71, P=0.005). The distribution of headings in test 1 also differed significantly from the training distribution (Watson–Williams test: $F_{1,64}$=6.7, P=0.005), confirming that the paths were deflected to the left by the displacement of the bar).

A possible mechanism to account for a subset of paths that may be guided by the displaced bar is that the ant has learnt how large a right turn it must make in order to face along the route. The path headings in the feeder direction could be guided from the starting channel purely idiothetically (e.g. Lent et al., 2009), or they may be guided idiothetically by path integration, as are *Drosophila* returning to a drop of sucrose that they have sampled (Kim and Dickinson, 2017). The individual paths of some ants do give an indication of guidance by path integration (Fig. S2).

In a second test (Fig. 2C, Fig. S1C), the bar was displaced to the right of its training position, with its right edge almost in line with the channel. Hartigan's dip test indicates that the distribution of path directions is unimodal. The mean path direction was shifted to the right of the training direction (mean heading: −22.8 deg, CI: −34.4 to −11.6), with a significant difference between the training and test 2 distributions (Watson–Williams test: $F_{1,50}$=13.7, P<0.001). The shift was partial such that the mean of the test 2 path distributions lay between the channel (0 deg) and bar-defined directions (−41.2 deg) and differed from both directions (Likelihood ratio test: channel direction: χ^2_1=10.46, P=0.001; bar-defined direction: χ^2_1=10.42, P=0.001). This compromise may be an example of ants averaging the directions of the outputs of independent navigational strategies (visual guidance and PI or idiothetic guidance) when the directions of the two outputs are relatively close (Collett, 2012; Wehner et al., 2016; Hoinville and Wehner, 2018).

In the last test, the bar was removed (Fig. 2D, Fig. S1D). With no bar, the path headings were more widely dispersed than in training (K-test for equal concentration parameters, F=6.5, P<0.001), but were not uniformly distributed around the entire circle. Again, the dip test indicates that the distribution is unimodal. The mean heading was 2.8 deg (CI: −35.7 to 45.8 deg) to the left of the feeder direction but did not differ significantly from it (Likelihood ratio test: χ^2_1=0.14, P=0.712). Similarly, the test 3 and training distributions did not differ significantly (Watson–Williams test: $F_{1,70}$=0.10, P=0.754). Cues from the channel alone may thus provide ants with some directional guidance along their route (cf. Lent et al., 2009).

Do the differences in path heading between treatments reflect the ants' reduced certainty about where to walk when the bar is missing or point to a different goal from the channel direction? We calculated for each ant a measure of path sinuosity as the ratio of the actual path to a direct one. In all cases, the sinuosity of the test trials was slightly greater than it was in training trials, but the difference was only significant for test 3, indicating that the routes taken by ants in tests with no bar are more circuitous than their training paths. The mean sinuosity of pre-test training runs of the tested ants was 2.79±0.12 (mean±s.e.m.). The mean sinuosity during the three tests was: test 1, 3.83±0.58; test 2, 3.02±0.33; test 3, 3.55±0.29. Paired t-tests using the mean sinuosity of each participating ant: training vs. test 1, t_{32}=1.67, P=0.104; training vs. test 2, t_{25}=0.201, P=0.842; training vs, test 3, t_{35}=2.94, P=0.006.

Facing directions at the endpoints of turns

The distributions of path directions (Fig. 2) indicate that the position of the bar has a major influence on the ants' direction of travel. Additional support for this suggestion comes from examining separately the endpoints of the right and left turns that ants make during their paths. We extracted two kinds of turn endpoints: (1) the maxima and minima in plots of the ants' facing directions (shown by circles in facing direction plots in Fig. 3); (2) turns that end in a plateau in which the ant keeps its facing direction steady for at least 0.2 s (visible as horizontal sections in the facing direction plots in Fig. 3), The two kinds of endpoints are combined in the histograms of Fig. 4.

Since the endpoints of turns made by the same ant may not be independent, statistical analyses relied on the circular mean of all endpoints over all the paths of each individual ant as the dependent variable. All the distributions of endpoints in pre-test training runs and test conditions were significantly non-uniform (Rayleigh's tests: pre-test training, Z=35.1, P<0.001; test 1, Z=20.8, P<0.001; test 2, Z=20.8, P<0.001; test 3, Z=3.33, P=0.035). Also, all the distributions were unimodal, according to Hartigan's dip tests (pre-test training, N=44, dip statistic=0.05, P=0.642; test 1, N=33, dip statistic=0.07, P=0.250; test 2, N=26, dip statistic=0.06, P=0.781; test 3, N=36, dip statistic=0.05, P=0.674). All the other endpoint distributions in Fig. 4 and subsequent figures were non-uniform and unimodal as shown by Rayleigh's and Hartigan's dip tests. To save space, the details are not reported. Because some distributions of endpoints are strongly skewed, the circular mean of the distribution is sometimes distant from the mode. Since all the distributions are statistically unimodal, we have sometimes adopted the mode (to within a 12 deg bin) as a measure of central tendency.

The distribution of all the endpoints during pre-test training trials (Fig. 4A) had a mean and mode of facing directions which almost coincide with the feeder direction and are very close to the mean of path directions in training (Fig. 2A). Indeed, the mean of all turn endpoints across all paths of each ant was generally correlated with the direction of the overall heading of the averaged paths (Fig. S4; circular correlation coefficient for pre-test training: ρ=0.77, P<0.001).

Similar correlations between paths and mean endpoints occurred in test trials (test 1, ρ=0.86, P<0.001, Fig. 4L; test 2, ρ=0.76, P=0.005; test 3, ρ=0.73, P<0.001). When left and right turns are combined, the mean discrepancies between mean endpoints and path headings were small and not significant (pre-test training, mean discrepancy=−1.4 deg, 95% CI=−6.7 to 3.8 deg, Likelihood ratio test: χ^2_1=0.20, P=0.652; test 1, mean discrepancy=−1.5 deg, 95% CI=−10.0 to 7.1 deg, Likelihood ratio test: χ^2_1=0.10, P=0.752; test 2, mean discrepancy=1.1 deg, 95% CI=−6.7 to 9.5 deg, Likelihood ratio test: χ^2_1=0.07, P=0.796; test 3, mean discrepancy=−1.3 deg, 95% CI=−13.2 to 10.7 deg, Likelihood ratio test: χ^2_1=0.03, P=0.871).

When turn endpoints during training were separated into left (Fig. 4D) and right (Fig. 4G) turns, the means, reflecting the skewed distributions, diverged to the left and right of the feeder direction and the pattern of correlations between path directions and mean endpoints shifted correspondingly (Fig. 4B,C). The modes, on the other hand, continued to align with the feeder direction (dashed vertical line), although the left turn mode is not prominent (Fig. 4D). Thus, like path directions, the endpoints of left turns in the feeder direction could be guided by idiothetic information, whereas right turn endpoints in the feeder direction could reflect idiothetic information or turns of learnt magnitude away from the bar. The latter possibility is supported by the pattern of right turn endpoints in test 1.

Journal of Experimental Biology (2021) 224, jeb242167. doi:10.1242/jeb.242167

When the bar was shifted to the left in test 1 (Fig. 4E), there was no clear mode. The mean of the left turn endpoints lay close to the bar-defined goal, corresponding to a leftward shift of the whole distribution and there was a component associated with the position of the bar, as was also the case in training (Fig. 4D). The mode of right turn endpoints remained aligned with the feeder direction and the mean shifted to a point close to the mode. Additionally, there was a small component of endpoints in the bar-defined goal direction.

To see whether these endpoints that are potentially guided by the bar are more than a chance phenomenon, we selected all right turns that began with the ant facing toward a point on the cylinder wall within ±20 deg of the centre of the bar. The mean of the distributions of these selected right turn end points during test 1 shifted significantly (leftwards $F_{1,60}$=5.59, P=0.003; Fig. 4K), compared with its companion, unselected endpoint distribution, while the pre-test training trials (Fig. 4J) showed a non-significant ($F_{1,85}$=1.77, P=0.187) trend toward a similar leftward shift.

The similarity of the two distributions of selected endpoints is emphasised by the following analysis. The means of the training and test 1 distributions were significantly different if, as usual, 0 deg in test 1 is taken to be the feeder direction (Watson–Williams test: test 1 vs. training: $F_{1,56}$=26.7, P<0.001). But the means did not differ if the test distribution is rotated so that the two are aligned on the position of the bar, making the bar-defined goal 0 deg for both distributions (Watson–Williams test: test 1 vs. training: $F_{1,56}$=0.269, P=0.606). The indistinguishable means of the two distributions suggest that in the case of the endpoints of turns that originated when the ant faced the bar, many of the ants' right turns were aimed at the bar-defined goal in training and in test 1.

Further evidence that ants may turn to the right by an angle that equals the angle between the bar and the goal comes from making the complementary selection; namely the origins of left and right turn endpoints that ended within ±20 deg of the bar-defined goal. In the sample of training (Fig. 5D) and test 1 (Fig. 5E) right turn endpoints, a sizeable cluster of turns started in a region close to the direction of the bar on the arena wall, though many turns originated from other points further away. Selected right turn endpoints in test 1 that ended in the feeder direction did not have a cluster of origins associated with the position of the bar (Fig. 5F).

In test 2 with the bar shifted rightwards, the mean of left turn endpoints is close to the feeder direction and those of right turns are well to the right of the feeder direction, but the modes of the right and left turn endpoint distributions coincide at about 20 deg to the right of the feeder direction (dashed vertical line Fig. 4F,I). This alignment may be a consequence of left and right turns sharing the same idiothetically defined goal.

Binocular ants

A re-analysis of an earlier study on binocular ants suggests that the findings on one-eyed ants apply to normal route following. In that study (Woodgate et al., 2016), wood ants were trained in the same apparatus to approach a goal with the direction set by a single bar placed to the left of the feeder direction and tested with wider bars. The major conclusion from various tests was that ants seemed to learn their route relative to the centre of mass of a shape.

We examine here the endpoints during pre-test training trials. The mean endpoints of left turns lay to the left of the feeder direction (mean=31.0 deg; 95% CI=16.7 to 47.6 deg; Likelihood ratio test: χ^2_1=7.71, P=0.006; Fig. 6A), as occurred in monocular ants (Fig. 4D). The mean of right turn endpoints lay non-significantly to the right of the feeder direction (mean=−17.0 deg; 95% CI=−31.5 to 0.4 deg; Likelihood ratio test: χ^2_1=2.20, P=0.138; Fig. 6B; cf. Fig. 4E for monocular ants). The peak of the distribution of left turn endpoints is close to the right edge of the black bar which lay at 30 deg from the feeder direction, perhaps reflecting left turns made to look at the bar. The origins of right turns that end within ±10 deg of the food direction also cluster close to the bar (Fig. 6D), supporting this suggestion.

Left turn endpoints that lay within ±10 deg or ±20 deg (Fig. 6C,E) of the feeder direction, as well as right turn endpoints within

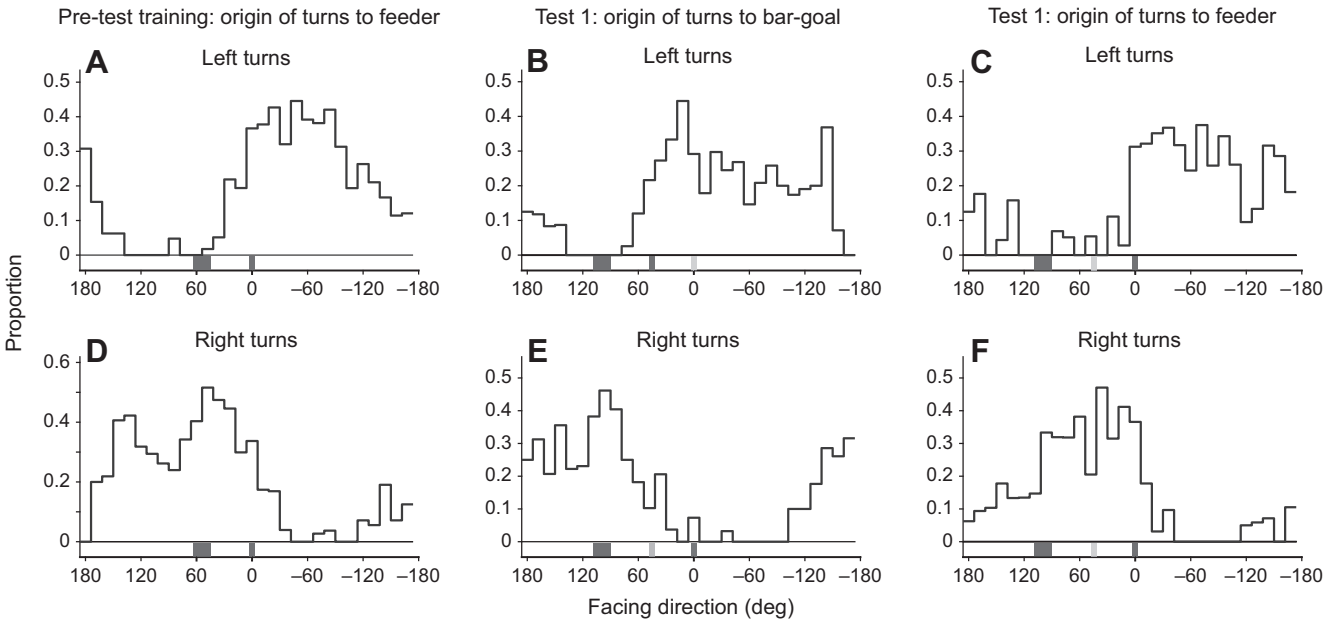

Fig. 5. The origins of left and right turns with endpoints close to a potential goal. Facing direction at the start of all turns that had endpoints within ±20 deg of the bar-defined or feeder directions during pre-test training runs and test 1. (A,D) Origins of left and right training endpoints that lay within ±20 deg of the feeder direction. Origins of left or right turn endpoints in test 1 that lay within ±20 deg of the bar-defined goal (B,E) or with endpoints within ±20 deg of the channel direction (C,F). Black line below panels shows feeder direction, grey line shows bar defined goal. Other conventions as in Figs 2 and 4.

Journal of Experimental Biology (2021) 224, jeb242167. doi:10.1242/jeb.242167

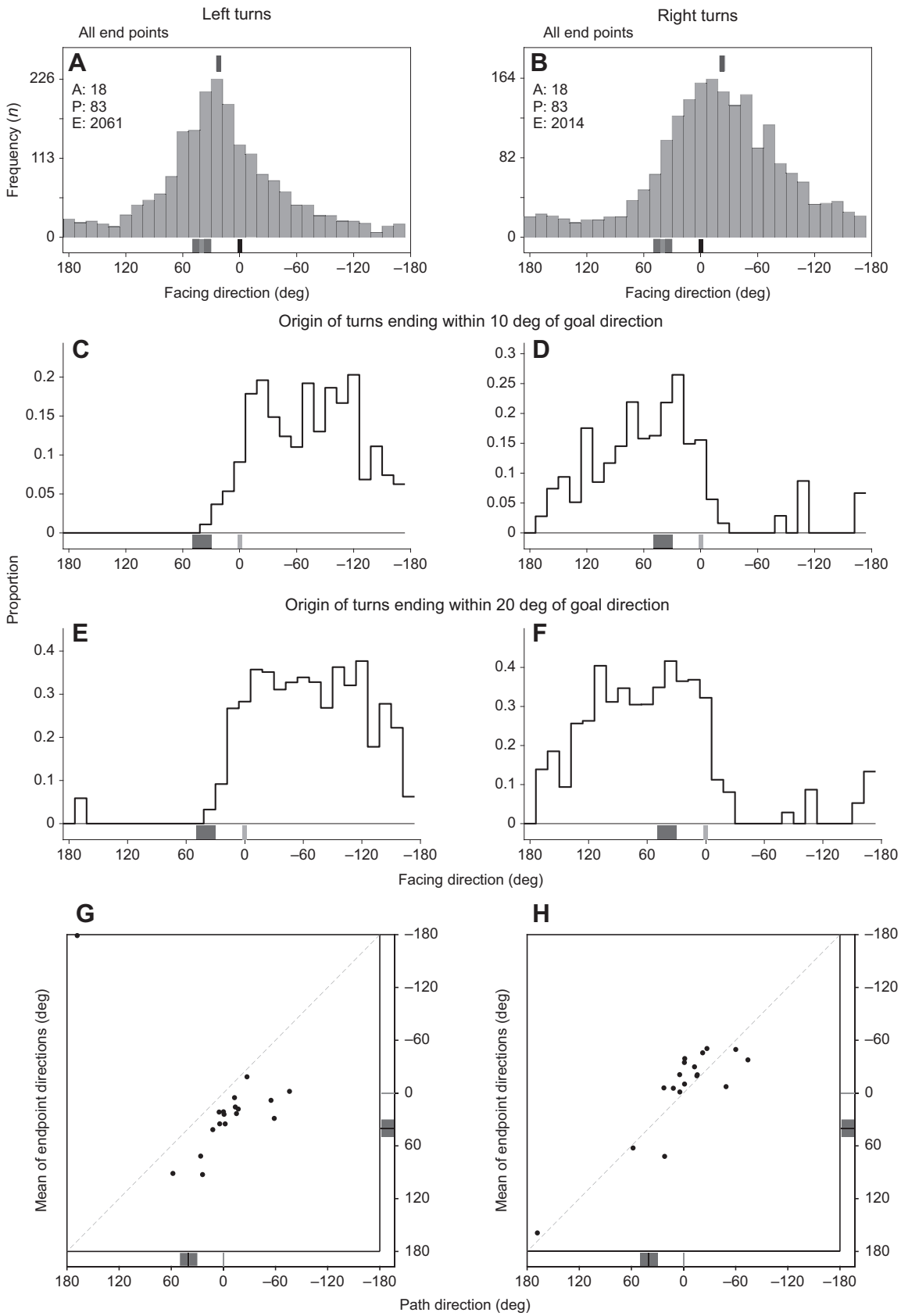

Fig. 6. Endpoints of turns in binocular ants during pre-test training runs. (A,B) Facing directions relative to food of all left (A) and right (B) turn endpoints in pre-test training runs. (C–F) Origins of left (C,E) and right (D,F) turns that ended within ±10 deg or ±20 deg of the feeder direction in pre-test training runs. (G,H) Scattergrams of the relation between an ant's mean path direction and the mean of all left turn (G) and right turn (H) endpoints across all the pre-test training trials of that each ant. Conventions as in Figs 4 and 5. Re-analysis of data from Woodgate et al. (2016).

Journal of Experimental Biology (2021) 224, jeb242167. doi:10.1242/jeb.242167

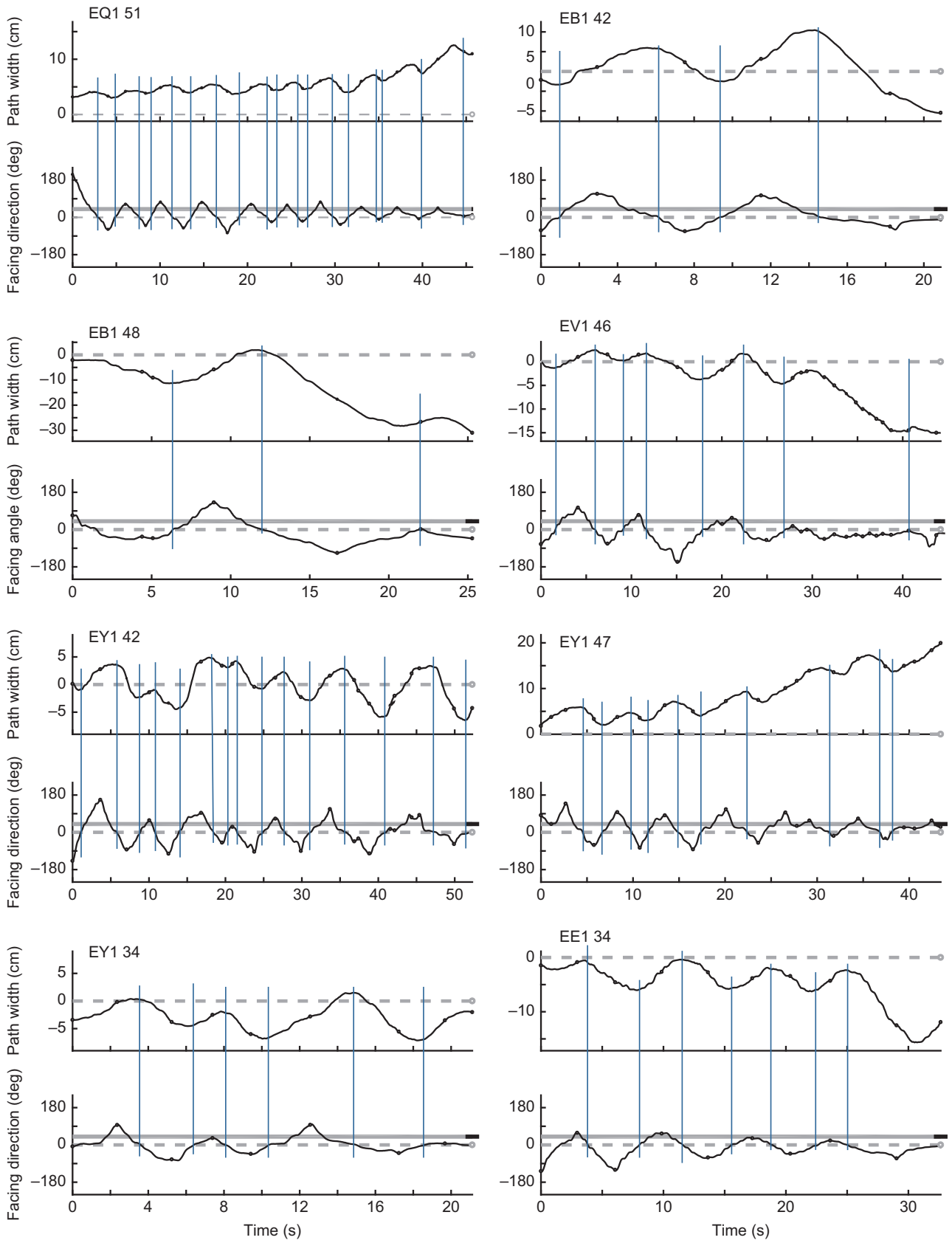

Fig. 7. Examples of zigzag paths in binocular wood ants. Each panel shows one path. Top traces show ant's position perpendicular to the direct path to the goal (path width) plotted against time. Bottom traces give the ant's facing direction relative to food over time. Grey solid line represents position of the bar on the retina as though ant were in the centre of the arena. In both panels, the horizontal grey dashed line shows the feeder direction. Continuous vertical blue lines joining the panels highlight points at which the ant is facing directly toward the food. These lines tend to intersect the inflection points in the trace of the ant's *y* position irrespective of the spatial or temporal regularity of the zigzag. Re-analysis of data in ants (each labelled by original ID codes used) from Woodgate et al. (2016).

±20 deg of the goal direction (Fig. 6F), seemed to originate from a broader range of directions and are likely to have a larger proportion of endpoints governed by path integration or alignment image matching. In the case of the origin of right turn endpoints, increasing the range of the sample from ±10 deg (Fig. 6D) to ±20 deg (Fig. 6F) included extra endpoints that masked the clustering around the bar associated with the ±10 deg range. This submergence of the cluster may indicate that visually guided turns from the bar to the goal are more precise than are idiothetic turns or alignment image matching operating in sparse visual surroundings. Taken as a whole, the data in Fig. 6 indicate that binocular ants, like monocular ones, rely to some degree on right turns linked to the bar for route guidance.

As in monocular ants (Fig. 4J,K), the means of endpoints of left and right turns were correlated with their associated path directions (circular correlation coefficients: left turns, ρ=0.76, P=0.016; right turns, ρ=0.71, P=0.036; Fig. 6G,H). While the slopes of left and right turns endpoints were the same, their offsets differed, so that left turn endpoints were shifted to the left of the path direction (mean discrepancy between endpoints and path heading=37.0 deg, 95% CI=27.7 to 47.2 deg; Likelihood ratio test: χ^2_1=25.50, P<0.001), while right turn endpoints did not differ significantly from path headings (mean discrepancy=−6.2 deg, 95% CI=−17.2 to 5.7 deg; Likelihood ratio test: χ^2_1=0.99, P=0.321). Again, like one-eyed ants, when left and right endpoints are combined, the means of all endpoints in each run did not differ significantly from the feeder direction (mean: 8.1 deg, CI=−6.6 to 24.4 deg; Likelihood ratio test: χ^2_1=0.59, P=0.444; Fig. S4B) and were correlated with the path headings (circular correlation coefficient: ρ=0.71, P=0.026; Fig. S4B).

Ants, as they travel along a path to the goal, tend to take a zigzag course that oscillates about the direct path. When a single visual feature is aligned with the route, ants tend to face in the route direction at the extrema of the zigzags (Lent et al., 2013). The same coincidence between goal facing and the zigzag path occurs here when the only visual features lies about 30 deg to the left of the direct route (Fig. 7, top trace). The bottom trace of each panel in Fig. 7 plots the ant's facing direction relative to the goal. When that is 0 deg, the ant is at an extremum of the zigzag path. Turns switch direction midway between the path extrema. The antiphase relation between turning and position within the zigzag seems to be independent of the frequency and regularity of the zigzag pattern.

DISCUSSION

Route navigation

Alignment image matching, the prevailing account of visually guided navigation in insects, suggests that an animal will turn until its current view matches a view learned when facing along the route and then move in that direction (Baddeley et al., 2012). In our study, that process could not operate because the left eye was painted over and the only visual cue when the ant faced in the correct direction was in the visual field of the blinded eye. The ant then saw no more than the white arena wall. This impediment did not prevent some ants from learning a route to a feeder. Moreover, when the visual cue was shifted in tests, the ants' paths were deflected in the appropriate direction, demonstrating that their movements were in part guided by the visual cue.

We propose that, during route learning, the size of right turns after turning to face the visual cue is guided by a knowledge of the route direction through idiothetic/path integration cues so that right turns can end with ants facing towards the goal. This turn size is then learnt and later applied when following the acquired route, thus providing support for alignment image matching. The recorded path in the current experiments was brief and the visual cue relatively distant so that assuming a single learnt turn size does not distort our conclusions. That would not be the case were the route longer. Just as views normally change along a route, so would the appearance or angular distance of any visual feature or cluster of features that could be used to control turn size.

A wood ant's path tends to oscillate with the desired goal direction faced at the inflection points of the oscillations or zigzags (Lent et al., 2013). This common oscillatory pattern is of particular benefit when keeping to an odour trail (Hangartner, 1969; Cardé and Willis, 2008; Willis et al., 2013; Namiki and Kanzaki, 2016). One-eyed ants zigzagging in the current experiments would see the bar during turns to the left, giving them an opportunity to acquire information to guide their subsequent routes. Indeed, the mean of the distribution of left turn endpoints is well to the left of the goal direction. Analysis of the endpoints of turns to the right indicate that, in the subset of turns that started with the bar in the ants' view, their direction was guided by the visual cue.

One puzzle that the data present is that although ants seem able to reach the goal using idiothetic cues without turning towards the bar, they mostly did not travel in the food direction when the bar was absent (Fig. 2D). A possible explanation comes from previous work on the expression of home and goal vectors that suggests that the vectors are not fully expressed if the surroundings in which they are tested differ markedly from the ant's accustomed surroundings (Cheung et al., 2012). It is possible that the bar provides a contextual, scene-setting cue as well as a cue for guidance.

That the original model of alignment image matching cannot be the whole story is also seen in the ability of ants (*Cataglyphis velox*) to drag large biscuit crumbs backwards along a familiar route (Schwarz et al., 2017; 2020a,b), with ants using terrestrial visual cues to guide their direction while facing backwards. It is proposed (Murray et al., 2020; Schwarz et al., 2020a) that ants travelling a route acquire two sets of views, one for each direction of travel, and that guidance becomes more precise when the two sets of view memories are co-active. One set is attractive and the other repulsive, with their valence switching with the ant's direction of travel. According to this model, ants motivated to travel to a food source or to go home do not just activate the appropriate set of view memories (Harris et al., 2005; Wehner et al., 2006). Instead, the motivational context determines which views are attractive and which repulsive.

The model also implies that a backward walking ant does not care that the locationally correct memories are viewed in the opposite order from that of acquisition. This implication must be reconciled with evidence that ants may learn a sequence of visual cues along a route and rely on sequential knowledge to help activate the currently appropriate view memory (Schwarz et al., 2020b). Wood ants learning laboratory routes from a starting point to a feeder reverse their travel direction for short stretches and obtain views on their outward trip that can guide their subsequent return trip (Graham and Collett, 2006). In this case, the sequence of memories for going home is only correct over the short distances of path reversal.

Separate neural systems for controlling alignment image matching and turn amplitude

Alignment image matching is likely to be mediated by the mushroom body (Ardin et al., 2016; Buehlmann et al., 2020; Kamhi et al., 2020) that can signal to other brain centres an attractive or aversive direction of travel (Aso et al., 2014). In contrast, controlled turns to or from memorised visual features are likely to be mediated by visuomotor processing in the central complex (CX) (Collett and Collett, 2018; Wystrach et al., 2020 preprint). Visual

learning of pattern orientation and elevation by *Drosophila* was originally shown to involve ring cells in the ellipsoid body (EB) and cells in the fan-shaped body of the CX (Liu et al., 2006; Pan et al., 2009). The experimental technique then available could not examine whether the azimuth of a visual stimulus is also memorised within these structures. This question has recently been resolved and suggests a clear division of responsibility between the mushroom body and the central complex in mediating different navigational strategies for route following.

First, a fly's heading direction is now known to reflect the position of a single 'bump' of electrical activity within the doughnut shaped EB (Seelig and Jayaraman, 2015). Secondly, the bump's position can be locked to a compass direction or to a visual stimulus (Seelig and Jayaraman, 2015; Turner-Evans et al., 2017; Green et al., 2017; Giraldo et al., 2018). Thirdly, studies of ring neurons in the EB and of EP-G neurons, which connect the EB and the protocerebral bridge (PB), explain how the bump of activity within the EB becomes linked to the direction of a visual cue (Fisher et al., 2019; Kim et al., 2019) and allows a facing direction within a visual scene to be rapidly associated with a particular compass direction, as might be needed for a visually controlled route.

The turn amplitudes that are likely to be mediated by known CX circuitry are of several kinds. Turns that place a visual stimulus in its expected position, like turns towards and away from the bar, can be understood in terms of the previous paragraph (Fisher et al., 2019; Kim et al., 2019; Green et al., 2019). Turns in the direction of a home vector are also likely to involve the CX, in this case, through interactions between the fan-shaped body, the PB and the EB (Neuser et al., 2008; Stone et al., 2017; Honkanen et al., 2019; Le Moël et al., 2019). Lastly, the lateral accessory lobes which contain neurons that mediate oscillatory changes in turn direction (Namiki and Kanzaki, 2016; Steinbeck et al., 2020) may control turns that switch direction in antiphase with the inflection points of zigzags (Fig. 7).

Acknowledgements
We thank the reviewers for many suggestions that materially improved this paper.

Competing interests
The authors declare no competing or financial interests.

Author contributions
Conceptualization: T.S.C.; Methodology: C.P., T.S.C.; Software: J.L.W.; Formal analysis: J.L.W., T.S.C.; Investigation: C.P., T.S.C.; Resources: T.S.C.; Data curation: J.L.W.; Writing - original draft: T.S.C.; Writing - review & editing: J.L.W., T.S.C.; Visualization: J.L.W., T.S.C.; Supervision: T.S.C.; Project administration: T.S.C.; Funding acquisition: T.S.C.

Funding
T.S.C. is grateful to the Leverhulme Trust for funding the project through an Emeritus Fellowship (EM-2016-066). J.L.W. was supported by Engineering and Physical Sciences Research Council program grant Brains-on-Board (EP/P006094/1).

References
Ardin, P., Peng, F., Mangan, M., Lagogiannis, K. and Webb, B. (2016). Using an insect mushroom body circuit to encode route memory in complex natural environments. *PLoS Comp. Biol.* **12**, e1004683. doi:10.1371/journal.pcbi.1004683

Aso, Y., Sitaraman, D., Ichinose, T., Kaun, K. R., Vogt, K., Belliart-Guérin, G., Plaçais, P.-Y., Robie, A. A., Yamagata, N., Schnaitmann, C. et al. (2014). Mushroom body output neurons encode valence and guide memory-based action selection in Drosophila. *eLife* **3**, e04580. doi:10.7554/eLife.04580.039

Baddeley, B., Graham, P., Husbands, P. and Philippides, A. (2012). A model of ant route navigation driven by scene familiarity. *PloS Comp. Biol.* **8**, e1002336. doi:10.1371/journal.pcbi.1002336

Berens, P. (2009). CircStat: a MATLAB toolbox for circular statistics. *J. Stat. Softw.* **31**, 1-21. doi:10.18637/jss.v031.i10

Buehlmann, C., Wozniak, B., Goulard, R., Webb, B., Graham, P. and Niven, J. E. (2020). Mushroom bodies are required for learned visual navigation, but not for innate visual behaviour in ants. *Curr. Biol.* **30**, 3438-3443. doi:10.1101/2020.05.13.094300

Çamlitepe, Y. and Stradling, D. J. (1995). Wood ants orient to magnetic fields. *Proc R. Soc.B* **261**, 37-41. doi:10.1098/rspb.1995.0114

Cardé, R. T. and Willis, M. A. (2008). Navigational strategies used by insects to find distant, wind-borne sources of odor. *J. Chem. Ecol.* **34**, 854-866. doi:10.1007/s10886-008-9484-5

Cheung, A., Hiby, L. and Narendra, A. (2012). Ant navigation: fractional use of the home vector. *PLoS ONE* **7**, e50451. doi:10.1371/journal.pone.0050451

Collett, M. (2010). How desert ants use a visual landmark for guidance along a habitual route. *Proc. Natl Acad. Sci. USA* **107**, 11638-11643. doi:10.1073/pnas.1001401107

Collett, M. (2012). How navigational guidance systems are combined in a desert ant. *Curr. Biol.* **22**, 927-932. doi:10.1016/j.cub.2012.03.049

Collett, M. and Collett, T. S. (2018). How does the insect central complex use mushroom body output for steering? *Curr. Biol.* **28**, R733-R734. doi:10.1016/j.cub.2018.05.060

Collett, T. S., Dillmann, E., Giger, A. and Wehner, R. (1992). Visual landmarks and route following in desert ants. *J Comp. Physiol. A* **170**, 435-442. doi:10.1007/BF00191460

Collett, M., Chittka, L. and Collett, T. S. (2013). Spatial memory in insect navigation. *Curr. Biol.* **23**, R789-R800. doi:10.1016/j.cub.2013.07.020

Fisher, N. I. (1995). *Statistical Analysis of Circular Data*. Cambridge University Press.

Fisher, Y. E., Lu, J., D'Alessandro, I. and Wilson, R. I. (2019). Sensorimotor experience remaps visual input to a heading-direction network. *Nature* **576**, 121-125. doi:10.1038/s41586-019-1772-4

Giraldo, Y. M., Leitch, K. J., Ros, I. G., Warren, T. L., Weir, P. T. and Dickinson, M. H. (2018). Sun navigation requires compass neurons in Drosophila. *Curr. Biol.* **28**, 2845-2852.e4. doi:10.1016/j.cub.2018.07.002

Golub, G. H. and Van Loan, C. F. (1996). *"Matrix Computations"*, 3rd edn., p. 596. The Johns Hopkins University Press.

Graham, P. and Cheng, K. (2009). Ants use the panoramic skyline as a visual cue during navigation. *Curr. Biol.* **19**, R935-R937. doi:10.1016/j.cub.2009.08.015

Graham, P. and Collett, T. S. (2006). Bi-directional route learning in wood ants. *J. Exp. Biol.* **209**, 3677-3684. doi:10.1242/jeb.02414

Green, J., Adachi, A., Shah, K. K., Hirokawa, J. D., Magani, P. S. and Maimon, G. (2017). A neural circuit architecture for angular integration in Drosophila. *Nature* **546**, 101-106. doi:10.1038/nature22343

Green, J., Vijayan, V., Mussells Pires, P., Adachi, A. and Maimon, G. (2019). A neural heading estimate is compared with an internal goal to guide oriented navigation. *Nat. Neurosci.* **22**, 1460-1468. doi:10.1038/s41593-019-0444-x

Hangartner, W. (1969). Structure and variability of the individual odor trail in *Solenopsis geminata* Fabr. (Hymenoptera, Formicidae). *Z. Vergl. Physiol.* **62**, 111-120. doi:10.1007/BF00298046

Harris, R. A., de Ibarra, N. H., Graham, P. and Collett, T. S. (2005). Priming of visual route memories. *Nature* **438**, 302. doi:10.1038/438302a

Hartigan, J. A. and Hartigan, P. M. (1985). The dip test of unimodality. *Ann. Stats.* **13**, 70-84. doi:10.1214/aos/1176346577

Hoinville, T. and Wehner, R. (2018). Optimal multiguidance integration in insect navigation. *Proc. Natl. Acad. Sci. USA* **115**, 2824-2829. doi:10.1073/pnas.1721668115

Honkanen, A., Adden, A., da Silva Freitas, J. and Heinze, S. (2019). The insect central complex and the neural basis of navigational strategies. *J. Exp. Biol.* **222**, jeb188854. doi:10.1242/jeb.188854

Jammalamadaka, S. R. and Sengupta, A. (2001). *Topics in Circular Statistics*, Vol. 5. World Scientific.

Kamhi, J. F., Barron, A. B. and Narendra, A. (2020). Vertical lobes of the mushroom bodies are essential for view-based navigation in Australian bull ants. *Curr. Biol.* **30**, 3432-3437.e3. doi:10.1016/j.cub.2020.06.030

Kim, I. S. and Dickinson, M. H. (2017). Idiothetic path integration in the fruit fly Drosophila melanogaster. *Curr. Biol.* **27**, 2227-2238.e3. doi:10.1016/j.cub.2017.06.026

Kim, S. S., Hermundstad, A. M., Romani, S., Abbott, L. F. and Jayaraman, V. (2019). Generation of stable heading representations in diverse visual scenes. *Nature* **576**, 126-131. doi:10.1038/s41586-019-1767-1

Kohler, M. and Wehner, R. (2005). Idiosyncratic route-based memories in desert ants, *Melophorus bagoti*: How do they interact with path-integration vectors? *Neurobiol. Learn. Memory* **83**, 1-12. doi:10.1016/j.nlm.2004.05.011

Le Moël, F., Stone, T., Lihoreau, M., Wystrach, A. and Webb, B. (2019). The central complex as a potential substrate for vector based navigation. *Front. Psychol.* **10**, 90. doi:10.3389/fpsyg.2019.00690

Lent, D. D., Graham, P. and Collett, T. S. (2009). A motor component to the memories of habitual foraging routes in wood ants? *Curr. Biol.* **19**, 115-121. doi:10.1016/j.cub.2008.11.060

Lent, D. D., Graham, P. and Collett, T. S. (2013). Phase-dependent visual control of the zigzag paths of navigating wood ants. *Curr. Biol.* **23**, 2393-2399. doi:10.1016/j.cub.2013.10.014

Liu, G., Seiler, H., Wen, A., Zars, T., Ito, K., Wolf, R., Heisenberg, M. and Liu, L. (2006). Distinct memory traces for two visual features in the *Drosophila* brain. *Nature* **439**, 551-556. doi:10.1038/nature04381

Mangan, M. and Webb, B. (2012). Spontaneous formation of multiple routes in individual desert ants (*Cataglyphis velox*). *Behav. Ecol.* **23**, 944-954. doi:10.1093/beheco/ars051

Mardia, K. V. and Jupp, P. E. (2009). *Directional Statistics*, Vol. 494. John Wiley & Sons.

Murray, T., Zoltán, K., Dahmen, H., Le Moël, F., Wystrach, A. and Zeil, J. (2020). The role of attractive and repellent scene memories in ant homing (*Myrmecia croslandi*). *J. Exp. Biol.* **223**, jeb210021. doi:10.1242/jeb.210021

Namiki, S. and Kanzaki, R. (2016). The neurobiological basis of orientation in insects: insights from the silkmoth mating dance. *Curr. Opin. Insect Sci.* **15**, 16-26. doi:10.1016/j.cois.2016.02.009

Narendra, A., Gourmaud, S. and Zeil, J. (2013). Mapping the navigational knowledge of individually foraging ants *Myrmecia croslandi*. *Proc. R. Soc. Lond. B* **280**, 20130683. doi:10.1098/rspb.2013.0683

Neuser, K., Triphan, T., Mronz, M., Poeck, B. and Strauss, R. (2008). Analysis of a spatial orientation memory in *Drosophila*. *Nature* **453**, 1244-1247. doi:10.1038/nature07003

Pan, Y., Zhou, Y., Guo, C., Gong, H., Gong, Z. and Liu, L. (2009). Differential roles of the fan-shaped body and the ellipsoid body in *Drosophila* visual pattern memory. *Learn. Mem.* **16**, 289-295. doi:10.1101/lm.1331809

Schwarz, S., Mangan, M., Zeil, J., Webb, B. and Wystrach, A. (2017). How ants use vision when homing backward. *Curr. Biol.* **27**, 401-407. doi:10.1016/j.cub.2016.12.019

Schwarz, S., Clement, L., Gkanias, E. and Wystrach, A. (2020a). How do backward-walking ants (Cataglyphis velox) cope with navigational uncertainty? *Anim. Behav.* **164**, 133-142. doi:10.1016/j.anbehav.2020.04.006

Schwarz, S., Mangan, M., Webb, B. and Wystrach, A. (2020b). Route-following ants respond to alterations of the view sequence. *J. Exp. Biol.* **223**, 218701. doi:10.1242/jeb.218701

Seelig, J. D. and Jayaraman, V. (2015). Neural dynamics for landmark orientation and angular path integration. *Nature* **521**, 186-191. doi:10.1038/nature14446

Steinbeck, F., Adden, A. and Graham, P. (2020). Connecting brain to behaviour: a role for general purpose steering circuits in insect orientation? *J. Exp. Biol.* **223**. jeb212332. doi:10.1242/jeb.212332

Stone, T., Webb, B., Adden, A., Weddig, N. B., Honkanen, A., Templin, R., Wcislo, W., Scimeca, L., Warrant, E. and Heinze, S. (2017). An anatomically constrained model for path integration in the bee brain. *Curr. Biol.* **27**, 3069-3085.e11. doi:10.1016/j.cub.2017.08.052

Turner-Evans, D., Wegener, S., Rouault, H., Franconville, R., Wolff, T., Seelig, J. D., Druckmann, S. and Jayaraman, V. (2017). Angular velocity integration in a fly heading circuit. *eLife* **6**, e23496. doi:10.7554/eLife.23496

Watson, G. S. and Williams, E. J. (1956). On the construction of significance tests on the circle and the sphere. *Biometrika* **43**, 344-352. doi:10.1093/biomet/43.3-4.344

Wehner, R., Michel, B. and Antonsen, P. (1996). Visual navigation in insects: coupling of egocentric and geocentric information. *J. Exp. Biol.* **199**, 129-140. doi:10.1242/jeb.199.1.129

Wehner, R., Boyer, M., Loertscher, F., Sommer, S. and Menzi, U. (2006). Ant navigation: one-way routes rather than maps. *Curr. Biol.* **16**, 75-79. doi:10.1016/j.cub.2005.11.035

Wehner, R., Hoinville, T., Cruse, H. and Cheng, K. (2016). Steering intermediate courses: desert ants combine information from various navigational routines. *J. Comp. Physiol. A* **202**, 459-472. doi:10.1007/s00359-016-1094-z

Willis, M. A., Ford, E. A. and Avondet, J. L. (2013). Odor tracking flight of male Manduca sexta moths along plumes of different cross-sectional area. *J. Comp. Physiol A* **199**, 1015-1036. doi:10.1007/s00359-013-0856-0

Woodgate, J. L., Buehlmann, C. and Collett, T. S. (2016). When navigating wood ants use the centre of mass of a shape to extract directional information from a panoramic skyline. *J. Exp. Biol.* **219**, 1689-1696. doi:10.1242/jeb.136697

Wystrach, A., Le Moel, F., Clement, L. and Schwarz, S. (2020). A lateralised design for the interaction of visual memories and heading representations in navigating ants. *bioRxiv* doi:10.1101/2020.08.13.249193

Zeil, J. (2012). Visual homing: an insect perspective. *Curr. Op. Neurobiol.* **22**, 285-293. doi:10.1016/j.conb.2011.12.008

Zollikofer, C. P. E., Wehner, R. and Fukushi, T. (1995). Optical scaling in conspecific *Cataglyphis* ants. *J. Exp. Biol.* **198**, 163. doi:10.1242/jeb.198.8.1637

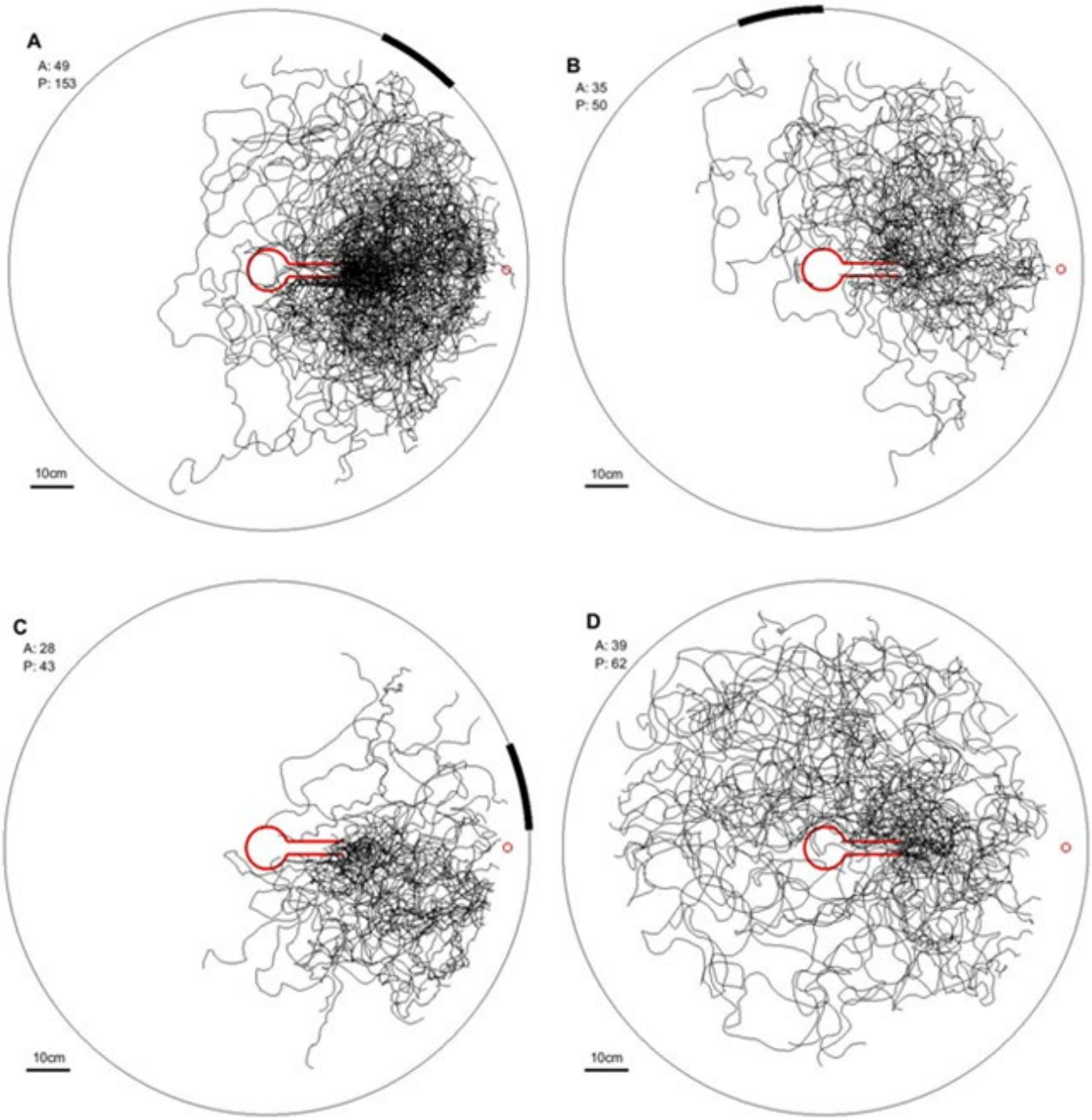

Fig. S1. Superimposition of ants' paths during training conditions and tests.

All paths in training trials just before a test and in tests 1-3 are shown superimposed without any filtering for consistency (See 'Exclusion of inconsistent ants' in Methods). **A:** paths recorded in pre-test training trials **B:** Paths in test 1 with bar shifted away from food. **C:** Paths in test 2 with bar shifted towards the food. **D:** Paths in test 3 with bar removed. In each panel, A gives the number of ants and P the number of paths.

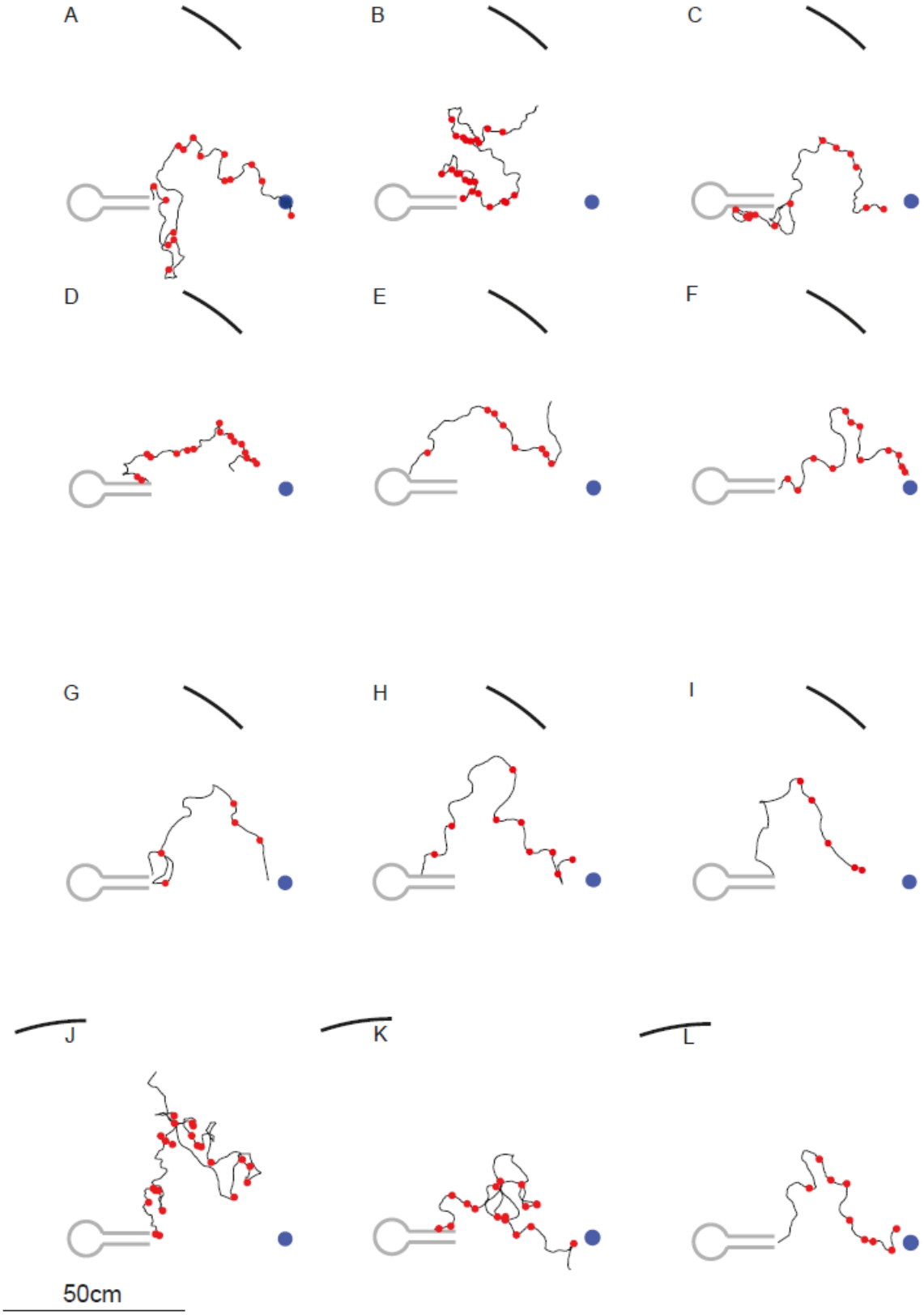

Fig. S2. Indications that ants can be guided by path integration to the food position.

A-L: Example paths in which ants turn to approach the food from directions other than the trained route. Path segments in which the ant's facing direction is within ±10^{o} of the feeder position are marked with red dots. Suggestive evidence for a food vector monitored through PI comes from examples of ants that leave the direct route to the goal and turn and travel towards the food when they are some distance from the trained path. Deviations from the trained path happen when ants head towards the bar. These deviant paths can be interrupted by the ant turning towards the goal and travelling in its direction. When the distance towards the goal is longer and is not just a brief interruption to a path elsewhere (examples A and H), facing the goal tends to occur at the peaks and troughs of a zigzag approach, as it does in binocular ants (Lent et al., 2013). Panels A-I come from training trials with a drop of sucrose at the goal. Could the ants obtain guidance cues from the sucrose, itself? During experiments over many years in this set up, ants show no signs of detecting the food until they have almost reached it. These concerns do not arise during tests in which food is always absent (see panels J-L). During all tracks shown, the bar remains within the field of the capped left eye while the ant turns and moves towards the food.

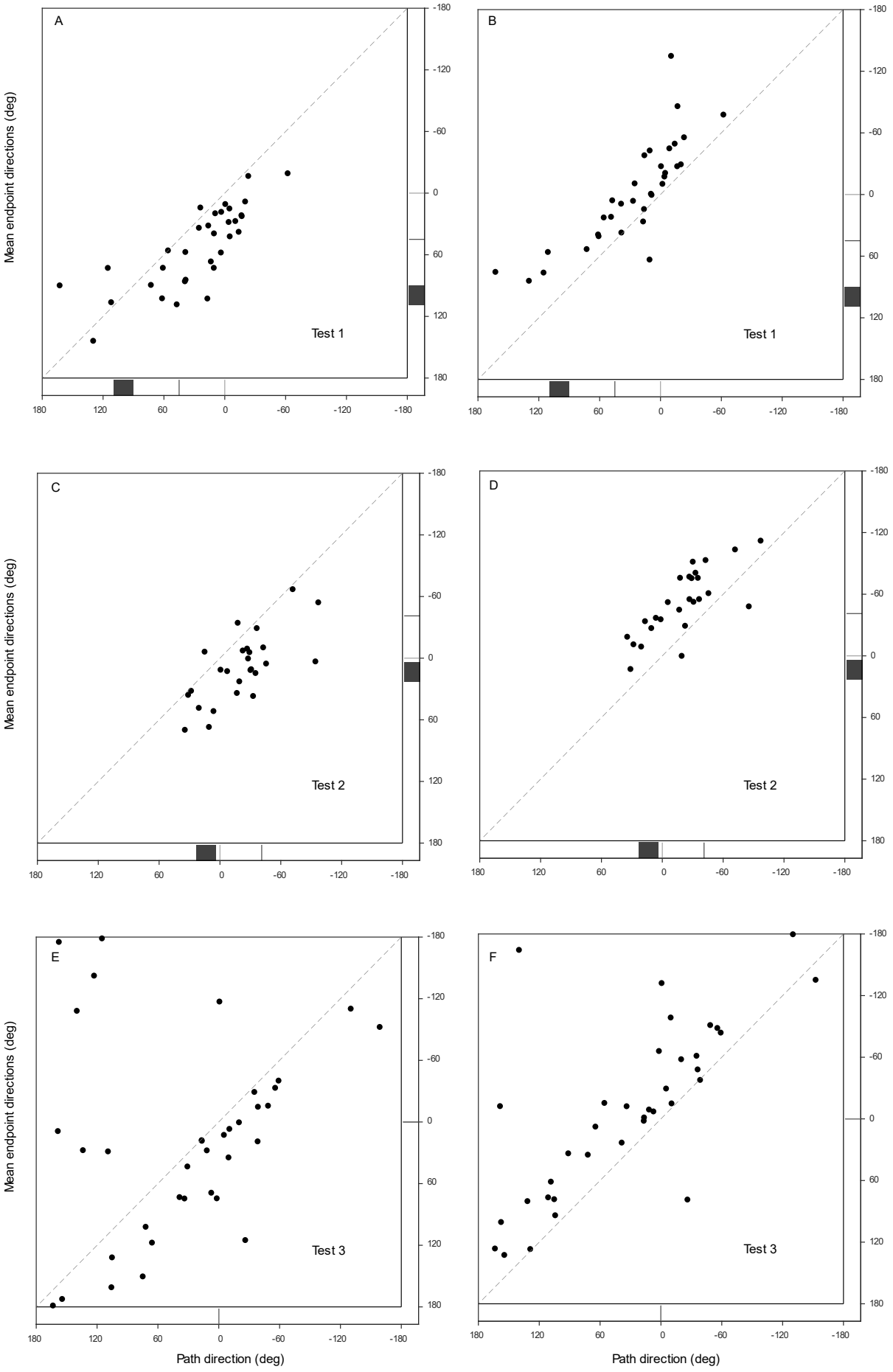

Journal of Experimental Biology • Supplementary information

Fig. S3. Correlations between the mean of all left or right endpoints made by each one-eyed ant and that ant's mean path direction during tests 1 to 3.

A, B: Test 1. A: Left turns: mean discrepancy between path heading and endpoint: 25.7° (CI: 16.8° to 25.5°; Likelihood ratio test: $\chi^2_1 = 18.8$, P <0.001; circular correlation coefficient: ρ = 0.82, P <0.001); B: right turns: mean discrepancy between path heading and endpoint: -28.0° (CI: -37.2° to -19.0°; Likelihood ratio test: $\chi^2_1 = 22.2$, P <0.001; circular correlation coefficient: ρ = 0.87, P <0.001). **C, D:** Test 2. C**:** Left turns: mean discrepancy between path heading and endpoint: 29.6° (CI: 19.7° to 39.1°; Likelihood ratio test: $\chi^2_1 = 22.4$, P <0.001; circular correlation coefficient: ρ = 0.70, P = 0.006); D: right turns: mean discrepancy between path heading and endpoint: -32.6° (CI: -40.4° to -24.1°; Likelihood ratio test: $\chi^2_1 = 30.9$, P <0.001; circular correlation coefficient: ρ = 0.77, P = 0.002). **E, F:** Test 3. E: Left turns: mean discrepancy between path heading and endpoint: 34.2° (CI: 20.8° to 47.5°; Likelihood ratio test: $\chi^2_1 = 12.4$, P <0.001; circular correlation coefficient: ρ = 0.55, P = 0.002); F: right turns: mean discrepancy between path heading and endpoint: -32.3° (CI: -43.6° to -21.6°; Likelihood ratio test: $\chi^2_1 = 15.8$, P <0.001; circular correlation coefficient: ρ = 0.77, P <0.001). Conventions as in Fig. 4 B, C.

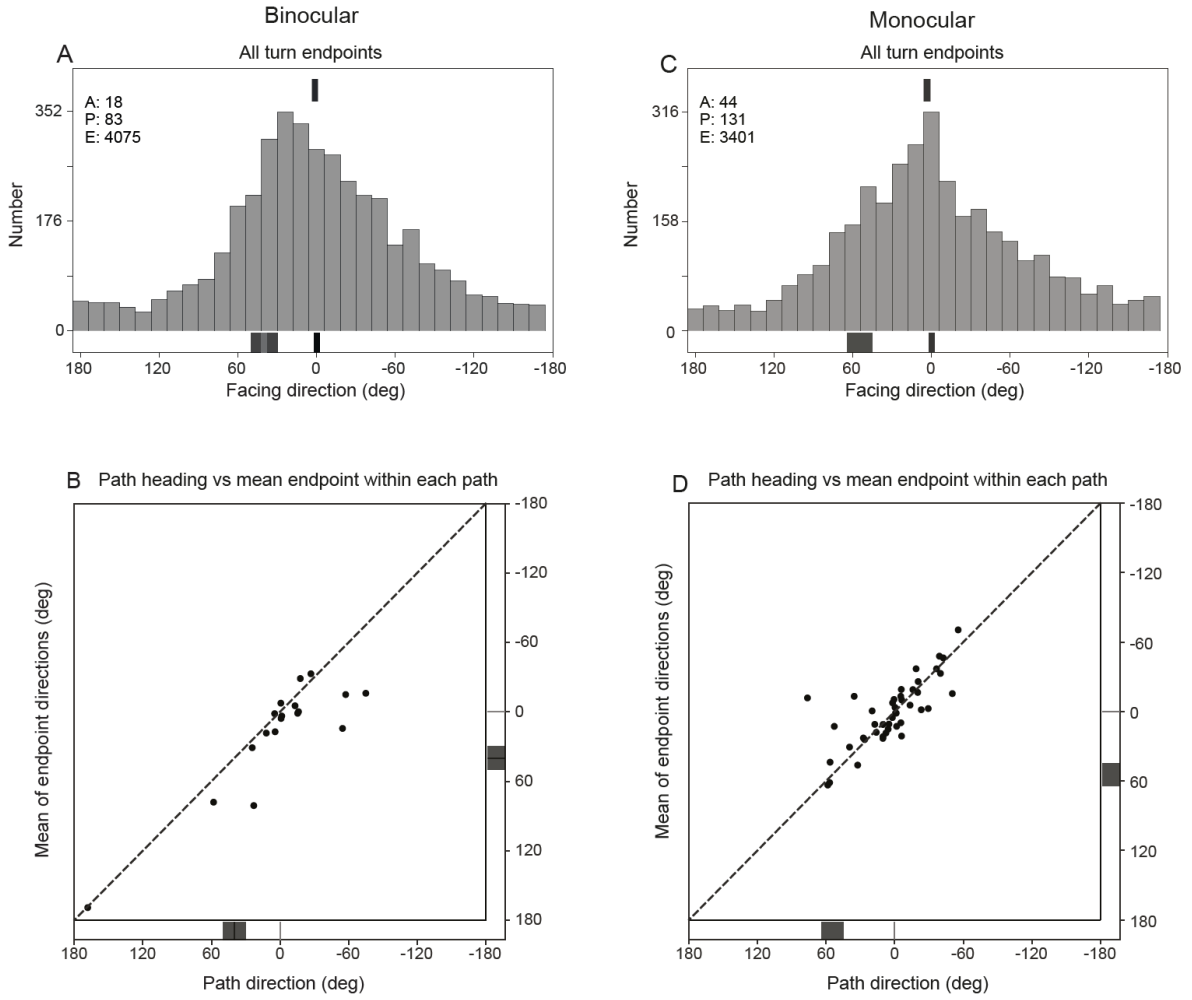

Fig. S4. Comparison between monocular and binocular ants of the endpoints of left and right turns combined during pre-test training.

A: Facing directions of binocular ants. Mean of the mean of all endpoints made by each ant does not differ from 0º (mean: 8.1º, CI = -6.6º to 24.4º; Likelihood ratio test: $\chi^2_1 = 0.59$, P = 0.444). **B:** Correlation between the mean of all endpoints made by each binocular ant and that ant's mean path heading (circular correlation coefficient: ρ = 0.71, P = 0.026). Mean endpoints were to the left of path headings (mean discrepancy = 16.0º, 95% CI = 5.6º to 27.1º; Likelihood ratio test: $\chi^2_1 = 6.41$, P = 0.011). **C**: Facing directions of monocular ants. Mean of the mean of all endpoints made by each ant does not differ from 0º (mean 0.99º (CI=-7.3º to 8.8º; Likelihood ratio test: $\chi^2_1 = 0.81$, P = 0.814). **D:** Correlation between the mean of all endpoints made by each monocular ant and that ant's mean path heading (circular correlation coefficient: ρ = 0.77, P <0.001). The mean discrepancy between endpoints and path headings is consistent with zero (mean discrepancy = 1.4º, 95% CI = -6.7º to 3.8º, Likelihood ratio test: $\chi^2_1 = 0.20$, P = 0.652). Details as in Fig. 4.

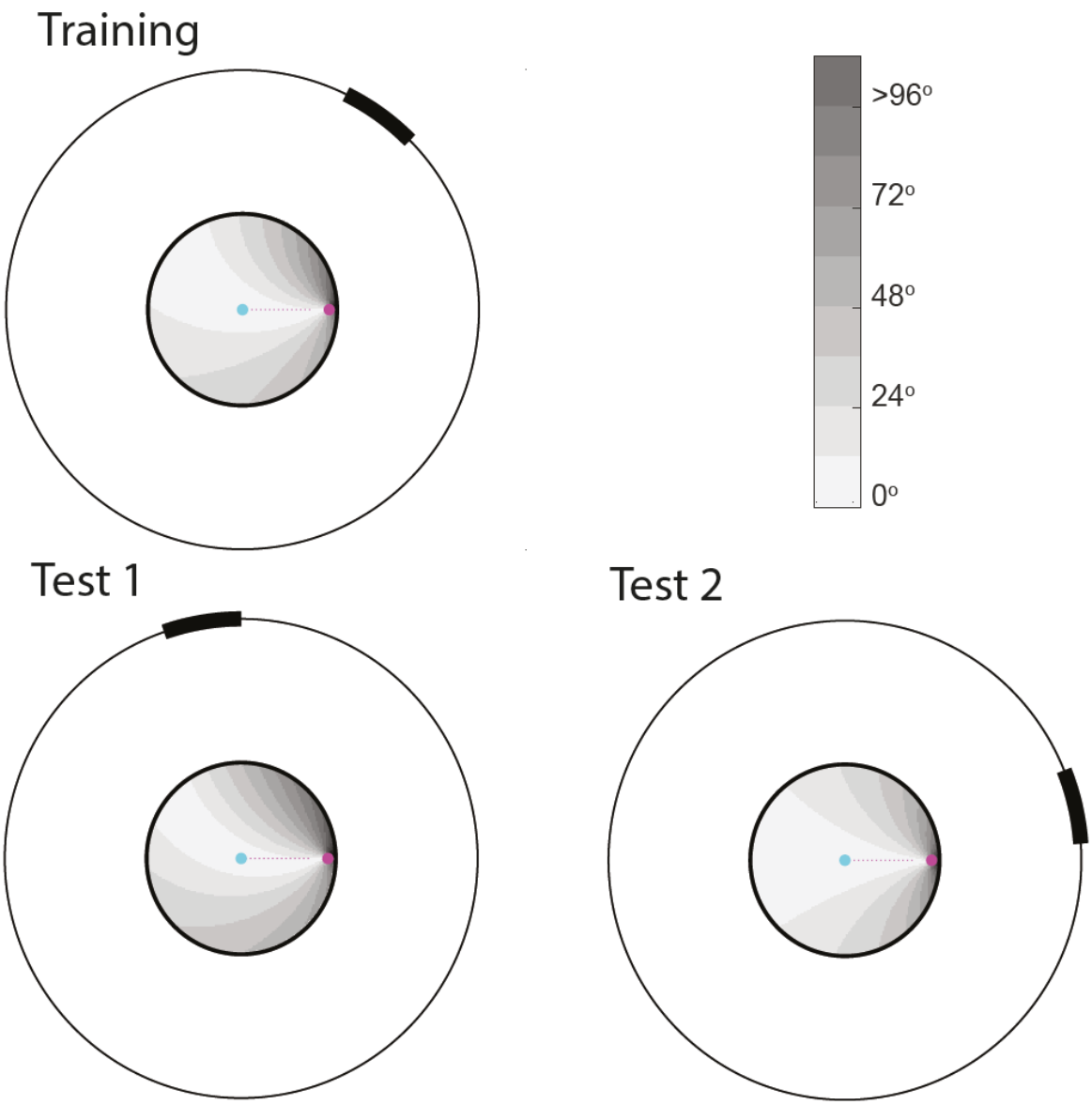

Fig. S5. Difference between the position of bar on retina of an ant in the centre of the arena and in other locations within the arena.

Outer ring: 180 cm diameter cylinder with vertical bar; inner ring 60 cm diameter arena. Differences are shown in |12°| steps shown in scale bar. Differences are small within the area in which ants follow routes (Figure S1).